Cancer Science
The official journal of the Japanese Cancer Association

Identification of drug candidate against prostate cancer from the aspect of somatic cell reprogramming

Takeo Kosaka,[1,7] Go Nagamatsu,[2,3,6,7] Shigeru Saito,[4,5,7] Mototsugu Oya,[1] Toshio Suda[2,6] and Katsuhisa Horimoto[4,6]

Departments of [1]Urology; [2]Cell Differentiation, The Sakaguchi Laboratory, School of Medicine, Keio University, Tokyo; [3]Precursory Research for Embryonic Science and Technology, Japan Science and Technology Agency, Kawaguchi, Saitama; [4]Molecular Profiling Research Center for Drug Discovery (molprof), National Institute of Advanced Industrial Science and Technology (AIST), Tokyo; [5]Chem and Bio Informatics Department, INFOCOM Corporation, Tokyo, Japan

(Received February 14, 2013/Revised April 10, 2013/Accepted April 16, 2013/Accepted manuscript online April 20, 2013/Article first published online May 26, 2013)

Considering the similarities between the transcriptional programming involved in cancer progression and somatic cell reprogramming, we tried to identify drugs that would be effective against malignant cancers. We used the early transposon Oct4 and Sox2 enhancer (EOS) system to select human prostate cancer (PCA) cells expressing high levels of OCT4. Patients with metastatic castration-resistant PCA that does not respond to treatment with docetaxel have few therapeutic options. The OCT4-expressing PCA cells selected using the EOS system showed increased tumorigenicity and high resistance to docetaxel, both *in vitro* and *in vivo*. By using their gene expression data, expression signature-based prediction for compound candidates identified an antiviral drug, ribavirin, as a conversion modulator from drug resistance to sensitivity. Treatment of PCA cells with ribavirin decreased their resistance against treatment with docetaxel. This indicated that ribavirin reversed the gene expression, including that of humoral factors, in the OCT4-expressing PCA cells selected using the EOS system. Thereby, ribavirin increased the efficacy of docetaxel for cancer cells. We propose a novel cell reprogramming approach, named drug efficacy reprogramming, as a new model for identifying candidate antitumor drugs. (*Cancer Sci* 2013; 104: 1017–1026)

The cells within a tumor are often heterogeneous with respect to proliferation kinetics, surface antigen expression, tumorigenicity and metastatic potential. Studies performed over the past few decades suggest that tumors are maintained by their own stem cells, the so-called cancer stem cells (CSC).[1–3] This 'CSC hypothesis' postulates that cancers are hierarchically organized and that only a single subset of cells, the CSC, drives cancer development and progression. However, the phenotypic plasticity of the cells within a tumor is likely to result in interconversion between a stem cell-like phenotype and a more differentiated phenotype.[4,5] This phenomenon is reminiscent of the dedifferentiation of somatic cells into induced pluripotent stem (iPS) cells. Takahashi and colleagues showed that overexpression of four transcription factors (4TF), OCT4, SOX2, KLF4 and c-MYC, induces pluripotency in somatic cells.[6,7] The iPS cells can differentiate into all three germ layers following appropriate induction. However, if these cells are introduced into animals, they can generate tumors in an undifferentiated state.[8,9] This suggests that some (or all) of the 4TF might enhance tumorigenicity in somatic cells.

The early transposon Oct4 and Sox2 enhancer (EOS) system is based on the transfection of a lentiviral-based promoter reporter (harboring GFP and a puromycin resistance gene), which is expressed under the control of the OCT4 and SOX2 enhancers,[10,11] into the cells of interest. OCT4, a POU transcription factor, is critical for somatic cell reprogramming.[12,13] Accumulating evidence suggests that OCT4 is involved in promoting tumorigenicity and malignancy in human cancers.[14–16] *OCT4* transcripts are consistently detected in human tumors and OCT4 is also expressed in CSC, including those of prostate cancer,[17,18] further implicating its participation in tumorigenesis and the development of an aggressive phenotype.[19–21]

Prostate cancer (PCA) is one of the most commonly diagnosed malignant tumors in men and is the second leading cause of cancer-related deaths in the United States.[22,23] One of the most difficult aspects of androgen-dependent PCA is that it almost inevitably progresses to a highly aggressive and life-threatening form, known as castration-resistant PCA (CRPC), after androgen ablation therapy. Although PCA treatments have improved over the years, taxanes remain the only effective form of chemotherapy.[24–26] However, taxane-based chemotherapy has limited beneficial effects in CRPC patients, extending life by several months at best. Therefore, it is important to develop more effective therapies that yield long-term improvements for CRPC patients.

The present study revealed that a human PCA cell line, which was enriched for cancer cells expressing high levels of OCT4 using the EOS system, showed strong resistance to chemotherapy and increased tumorigenicity when transplanted into nude mice. The gene expression patterns of these EOS-selected cancer cells were then analyzed and compared using the Broad Institute's Connectivity Map (http://www.broadinstitute.org/cmap) to identify candidate drugs with the potential to revert an inverse gene signature pattern. The Connectivity Map identified a candidate drug, ribavirin, as capable of reverting docetaxel-resistant PCA cells selected using the EOS system. Ribavirin treatment reverted the gene expression profiles from EOS to PGK selected, especially cell cycle regulators and humoral factors. Furthermore, ribavirin treatment increased drug sensitivity to docetaxel. The reprogramming phenomenon achieved the characteristic gene expression profiles and functional phenotypes. In the present study, ribavirin treatment of EOS cells converted the gene expression profiles and the tumor malignant phenotypes to the non-selected state.[27,28] The concept underlying this strategy is similar to that involved in other reprogramming technologies. We call this new method drug efficacy reprogramming (DER).

[6]To whom correspondence should be addressed.
E-mails: gonag@z2.keio.jp; sudato@z3.keio.jp; k.horimoto@aist.go.jp
[7]These authors contributed equally to this work.

doi: 10.1111/cas.12183

Materials and Methods

Cell lines and culture. DU145 and LNCaP PCA cells were routinely maintained in RPMI-1640 (Invitrogen, Carlsbad, CA, USA), supplemented with 10% FBS, at 37°C in a humidified atmosphere containing 5% CO_2. The DU145 and LNCaP cell lines were obtained from the American Type Culture Collection (Manassas, VA, USA) (HTB-81 and CRL-1740, respectively). The PGK and EOS lentiviruses were generated using HEK293T cells, as described previously.[29]

Immunocytochemistry. The tissue sections were incubated with an anti-OCT4 rabbit polyclonal antibody (1:500 dilution; Abcam, Cambridge, UK) at room temperature for 1 h. Avidin–biotin complex peroxidase methods were used. To evaluate OCT4 staining, cancer cells with positive nuclear staining were counted in at least 10 representative fields and the mean percentage of OCT4-positive cancer cells and the staining intensity, which ranged from 0 to 3 (0, none; 1, minimal; 2, medium; 3, strong) were estimated using a semi-quantitative scoring system.

Xenograft tumorigenicity assay. DU145-PGK, DU145-GFP, sh-OCT4 DU145-EOS and sh-luci DU145-EOS cells were harvested, washed in PBS and resuspended in Matrigel (BD Biosciences, San Jose, CA, USA). The cells (10^3 or 10^4) were then injected subcutaneously into 6-week-old BAL B/C nude mice. Tumors were measured every 5 days after injection.

Cell viability assay. DU145 and LNCaP cells were plated in 96-well plates, allowed to attach for 24 h and then treated with different concentrations of docetaxel. A water-soluble tetrazolium (WST) reagent (Takara Bio Inc., Shiga, Japan) was added to each well for 1 h. Cell viability was estimated using colorimetry at 570 nm.

Mouse xenograft model for drug testing. DU145-PGK and DU145-EOS cells were injected into nude mice for docetaxel testing. One million DU145-PGK- or EOS-selected cells formed detectable tumors within 1–2 weeks of injection. The tumors were measured every 5 days. When the tumor volume reached approximately 200 mm^3, the mice were assigned into one of two groups: a control group or a docetaxel-treated group. Docetaxel (10 mg/kg) was injected i.p. on day 1. For the ribavirin tests, ribavirin (40 μg/kg per day) in 0.5% carboxymethyl cellulose was administered p.o. every day from day 1. A carboxymethyl cellulose solution was administered as a control. The mice were assigned to one of six groups (n = 6–8 mice) when the mean tumor volume reached approximately 200 mm^3: a non-treated control group; docetaxel only (10 mg/kg); docetaxel only (5 mg/kg); docetaxel (10 mg/kg) plus ribavirin (40 μg/kg per day), per os (p.o.); docetaxel (5 mg/kg) plus ribavirin (40 μg/kg per day, p.o.); or ribavirin only (40 μg/kg per day, p.o.). The ribavirin treatments were done from day 1 to 15. Daily oral administration of ribavirin yields a mean body concentration of approximately 1 μM and is well tolerated and non-toxic to mice.[30]

Real-time quantitative PCR. Total RNA was isolated using an RNeasy Mini kit (Qiagen, Hilden, Germany). RNA was reverse transcribed into cDNA using a High Capacity cDNA Archive kit (Applied Biosystems, Carlsbad, CA, USA). The reaction mixture (1 μL) was then used as a template in a TaqMan Fast real-time quantitative PCR assay, performed using the 7500 Fast Real-time PCR system (Applied Biosystems). Primers and TaqMan probe sets (TaqMan Gene Expression Assays) for human *OCT-4, c-MYC* and *GAPDH* were purchased (Applied Biosystems, Carlsbad, CA, USA).

Knockdown and overexpression of OCT4. The following shRNA sequence was used for the *OCT4* knockdown: 5′-GGATGTGGTCCGAGTGTGGTTCAAGAGACCACACTCGG ACCACATCCTTTTTT-3′.[31] The following shRNA sequence targeted to luciferase was used as a control:5′-GTGCGTTG CTAGTACCAACTTCAAGAGAGTTGGTACTAGC AACGCAC TTTTTTACGCGT-3′. The sequences were introduced into the pSIREN-RetroQ-DsRed-Express lentiviral vector (Clontech, Palo Alto, CA, USA). Virus production and infection were performed as previously described.[29] Infected cells were sorted based on DsRed-Express fluorescence using a FACSAria II cell sorter (BD Biosciences, San Jose, CA, USA).

To overexpress *OCT4*, the gene encoding human *OCT4* was PCR cloned, inserted into the pGEM-T-easy plasmid (Promega, Madison, WI, USA) and then inserted into the pMXs-IRES-GFP retroviral vector via the *Bam*HI and *Xho*I sites. The PCR primers used were: OCT4, forward 5′-GGATCCGC CACCATGG CGGGACACCTGGCTTCGGAT-3′; and OCT4, reverse 5′-GTC GACTCAGTTTGAATGCATGGGAGAGCC-3′. Virus production and infection were performed as previously described.[29] Infected cells were sorted by GFP fluorescence using a FACSAria II cell sorter (BD Biosciences, San Jose, CA, USA).

Microarray analyses. Gene expression profiles of PGK, EOS-selected cells and ribavirin-treated cells were analyzed using the whole human genome Affymetrix HG-U133 Plus 2 microarray (Affymetrix, Santa Clara, CA, USA). RNA target preparation for microarray expression analysis was performed according to the manufacturer's protocol using a GeneChip(R) 3′ IVT Express kit (Affymetrix). The entire process is briefly described as follows. One hundred nanograms of total RNA were converted into a double-stranded cDNA template for transcription. Transcription was performed *in vitro* to synthesize the amplified RNA (aRNA) and to incorporate a biotin-conjugated nucleotide. After purification and fragmentation of the aRNA, a 12.5 μg portion was hybridized to the GeneChip (R) Human Genome U133 Plus 2.0 Array (Affymetrix). The array was incubated for 16 h at 45°C and then automatically washed and stained with the GeneChip(R) Hybridization, Wash and Stain kit (Affymetrix). The Probe Array was scanned using a GeneChip(R) Scanner, model 3000 7G.

The measured data were normalized using the MAS5.0 method and the R Bioconductor 'affy' package. Hierarchical clustering was performed with the Euclidean distance coefficient and the UPGMA method (using the R 'hclust' package and Java TreeView 1.1.0) to illustrate the differences in the global gene expression patterns between PGK and EOS cells.

To obtain potential compounds that could reprogram the gene expression of the PGK and EOS cells, first the PGK-EOS gene signature was estimated by calculating the twofold change in the mean expression and then the probe list in the PGK-EOS signature was entered into the Connectivity Map (http://www.broadinstitute.org/cmap/). Note that the top 500 upregulated and downregulated probes, which are compatible with the HG-U133A platform, were used according to the Connectivity Map system. The threshold of significance for the candidate compounds was set at $P < 0.05$.

After identifying the most plausible candidate, to demonstrate the reprogramming effect by the candidate, a principal component analysis for the PGK-EOS signature was further performed using the PCA node in the KNIME 2.5.2 workflow platform.

The pathway analysis was performed as follows. First, the genes with average expression differences of at least twofold between PGK and EOS in DU145 and LNCaP cells were selected as the significantly expressed gene signature. The signature for ribavirin treatment was then calculated using the same procedure. Second, an enrichment analysis was applied for the gene signatures to the canonical pathway gene stets (c2.cp.v3.0.entrez) in the molecular signature database (http://www.broadinstitute.org/gsea/msigdb). The enrichment probability of the gene list was then estimated based on the hypergeometric probability as follows. When a target gene set

doi: 10.1111/cas.12183

is composed of k genes and l genes are included in the target set, the probability is obtained by:

$$P(X \leq l) = 1 - \sum_{i=0}^{l} \frac{\binom{M}{i}\binom{N-M}{k-i}}{\binom{N}{k}},$$

where M is the number of genes in the target set and N is the total number of genes in all gene sets. Thereafter, the false discovery rate is estimated using the Benjamini–Hochberg procedure. In the present study, we selected enriched gene sets with a false discovery rate <5%.

Results

Application of the EOS enhancer selection system for the enrichment of PCA cells. The current methods of stratifying PCA to predict outcomes are based on clinicopathological factors, including the Gleason score and prostate-specific antigen levels.[22,23] Although they are helpful, these parameters are not sufficient. This has prompted the development of genetic and biological approaches to analyze PCA progression, with the goal of identifying biomarkers that might lead to improved patient management and the identification of new therapeutic targets. We used the EOS selection system, which was designed to purify human iPS cells,[10,11] to enrich tumor cells showing high OCT4 expression. The EOS vector contains GFP and puromycin resistance genes, with expression driven by the Oct4 and Sox2 enhancers. The EOS vector is transduced into DU145 cells, which are then selected with puromycin. A vector containing a ubiquitous PGK promoter, which drives the expression of GFP and the puromycin resistance gene, is used as a control. A quantitative PCR (qPCR) analysis of RNA extracted from the transformed cells confirmed that DU145-EOS cells showed significantly higher ($P < 0.01$) levels of *OCT4* mRNA expression than DU145-PGK cells (Fig. 1a). Furthermore, an immunocytochemistry analysis indicated the enrichment of OCT4-expressing cells using EOS selection (Fig. S1).

Next we analyzed the tumorigenicity of DU145-EOS and DU145-PGK cells (Fig. 1b). Four nude mice were injected with either DU145-EOS or DU145-PGK cells (10^4 cells per mouse). Three out of the four mice developed detectable tumors within 8 weeks of the primary injection, while no tumors were detected in the mice injected with DU145-PGK cells during the 12-week observation period. The same results were observed when mice were injected with 10^3 cells (Fig. 1b). H&E staining of the tumors was also performed

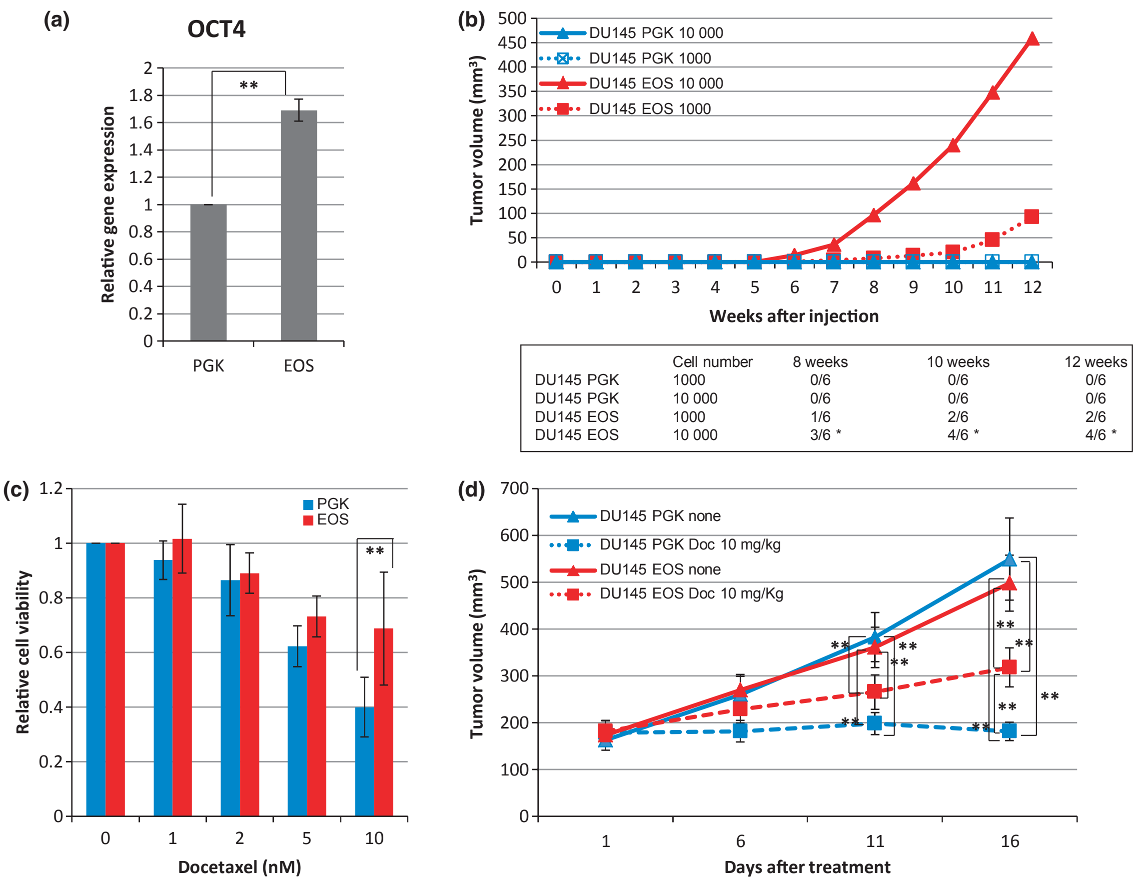

Fig. 1. Increased expression of OCT4 and enhanced tumorigenicity of early transposon Oct4 and Sox2 enhancer (EOS)-selected DU145 cells. (a) Quantitative PCR analysis of OCT4 mRNA expression in DU145-PGK and DU145-EOS cells. Relative expression is shown (mean ± SD; $^{**}P < 0.01$). (b) *In vivo* tumor formation in mice injected with DU145-PGK or DU145-EOS cells. Tumor volumes were calculated at the indicated time points (upper panel) and the number of tumors is shown in the lower panel (Mann–Whitney U-test; $^{*}P < 0.05$). (c) DU145-PGK and DU145-EOS cells were treated with increasing concentrations of docetaxel *in vitro* and cytotoxicity was measured using a water-soluble tetrazolium assay. The viability of treated cells was calculated relative to that of untreated controls (mean ± SD; $^{**}P < 0.01$). (d) *In vivo* sensitivity to docetaxel. DU145-PGK- and DU145-EOS cells (1×10^6) were injected into nude mice. Mice ($n = 6$) were treated with or without docetaxel (10 mg/kg). Mean tumor volumes are shown at the indicated time points (mean ± SD; $^{**}P < 0.01$).

(Fig. S2). It is noteworthy that an injection containing only 10^3 DU145-EOS cells promoted tumor formation. These results confirmed that DU145-EOS cells were more tumorigenic than DU145-PGK cells.

The high OCT4 expression by human PCA cells suggests that they might have strong resistance to anticancer agents. To examine this possibility, we used the cytotoxic drug docetaxel, which is currently approved for the treatment of CRPC. The results of an *in vitro* WST cell viability assay revealed that DU145-EOS cells were more resistant to docetaxel than DU145-PGK cells (Fig. 1c). Next we examined whether this was also the case *in vivo*. One million DU145-PGK or DU145-EOS cells were injected into castrated nude mice to initiate tumor formation. The mice were then treated with docetaxel or vehicle and tumor growth was examined. The DU145-PGK tumors that developed in the docetaxel-treated group were much smaller than those that developed in the non-treated group (Fig. 1d). However, the DU145-EOS tumors that developed in the docetaxel-treated mice were only slightly smaller than those that developed in the non-treated mice. These results indicate that DU145-EOS cells are more resistant to treatment with docetaxel.

Docetaxel resistance is mediated by high OCT4 expression. We then analyzed the effects of high OCT4 expression on chemoresistance by knocking down *OCT4* expression in DU145-EOS cells (Fig. 2a–c) and by overexpressing *OCT4* in non-EOS-selected cells (Fig. 2d–f). An *OCT4*-specific sh-RNA sequence was introduced into EOS-selected cells to knockdown *OCT4* expression.[31] The same procedure was performed using a *luciferase*-specific sh-RNA sequence as a control. A qPCR analysis revealed that *OCT4* sh-RNA-treated cells (DU145-EOS$^{sh\text{-}OCT4}$) showed a significant reduction in *OCT4* expression (Fig 2a). Although mice injected with DU145-EOSsh-OCT4 cells did not exhibit tumors, the *Luciferase* knockdown DU145-EOS (DU145-EOSsh-Luci) control cells formed detectable tumors during the 12 weeks of observation (Fig. 2b). H&E staining of the tumors was also performed (Fig. S2). We then compared the *in vitro* docetaxel sensitivities of DU145-EOS$^{sh\text{-}OCT4}$ and DU145-EOS$^{sh\text{-}Luci}$ with that of DU145-EOS using a WST cell viability assay. DU145-EOS$^{sh\text{-}OCT4}$ cells were significantly more

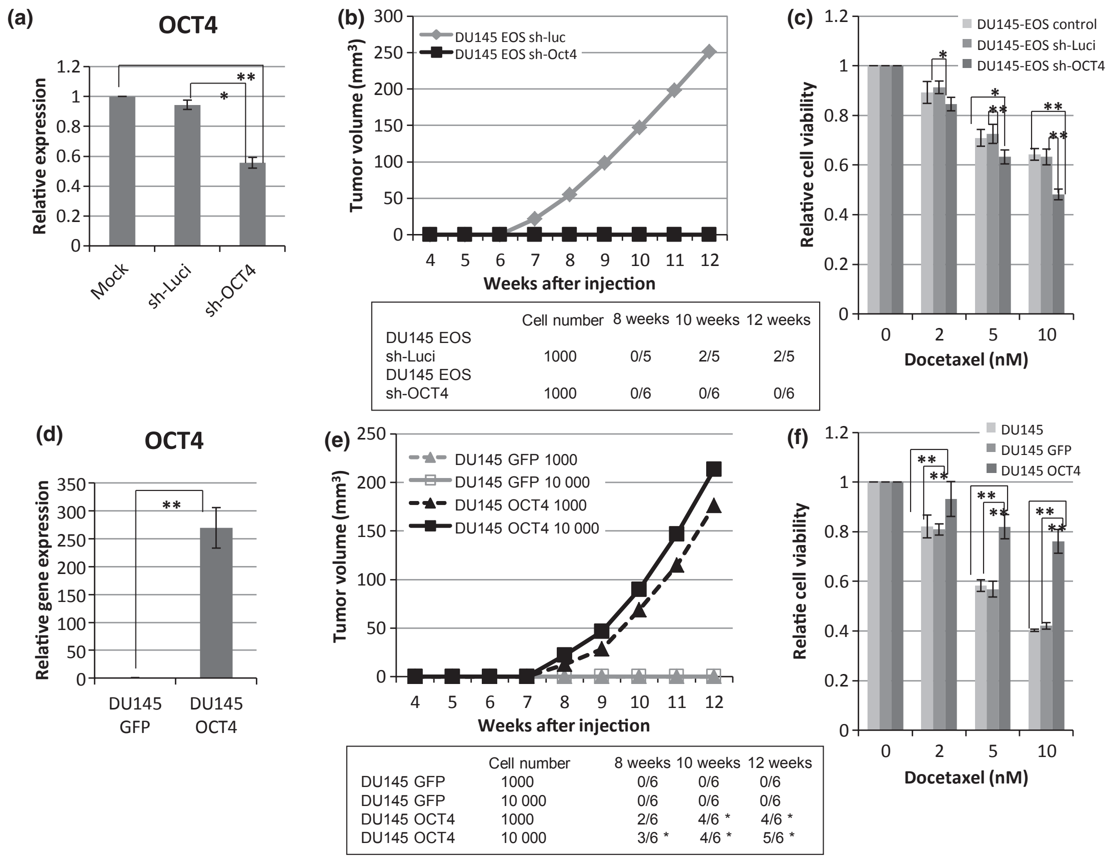

Fig. 2. High OCT4 expression increases the malignancy of DU145 cells. (a) Quantitative PCR analysis of OCT4 mRNA expression after transduction of sh-RNA targeting luciferase (DU145-EOS sh-Luci) or OCT4 (DU145-EOS sh-OCT4). Relative expression levels are shown (mean ± SD; $*P < 0.05$, $**P < 0.01$). (b) *In vivo* tumor formation following OCT4 knockdown. DU145-EOS sh-Luci or DU145-EOS sh-OCT4 (1000 or 10 000 cells) were inoculated into nude mice. Tumor volumes were calculated at the indicated time points (upper panel) and the number of tumors is shown in the lower panel. (c) *In vitro* sensitivity of DU145-EOS sh-Luci or DU145-EOS sh-OCT4 to docetaxel. The viability of DU145-EOS, DU145-EOS sh-Luci and DU145-EOS sh-OCT4 was determined in a water-soluble tetrazolium (WST) assay. The viability of the treated cells was calculated relative to that of untreated controls (mean ± SD; $*P < 0.05$, $**P < 0.01$). Forced expression of OCT4 in DU145 (DU145-OCT4) cells (d–f). (d) Quantitative OCT4 mRNA analysis after the introduction of a vector containing GFP alone or a vector containing OCT4-GFP. Relative expression levels are shown (mean ± SD; $**P < 0.01$). (e) *In vivo* tumor formation following the injection of nude mice with 1000 or 10 000 DU145-GFP or DU145-OCT4 cells. Tumor volumes were calculated every 5 days and the number of tumors was determined (lower panel) (Mann–Whitney *U*-test; $*P < 0.05$). (f) DU145-GFP and DU145-OCT4 cells were treated with the indicated concentrations of docetaxel. Cytotoxicity was measured using a WST assay and the viability of treated cells was calculated relative to that of the untreated controls (mean ± SD; $**P < 0.01$). EOS, early transposon Oct4 and Sox2 enhancer.

doi: 10.1111/cas.12183

sensitive to docetaxel than DU145-EOS$^{sh\text{-}Luci}$ or DU145-EOS cells (Fig. 2c).

For the OCT4 gain-of-function analysis, a GFP vector (DU145-GFP) or an OCT4-GFP vector (DU145-OCT4) was introduced into non-EOS-selected DU145 cells (Fig. 2d–f). The forced expression of *OCT4* in non-selected cells led to increased tumorigenicity (Fig. 2e). H&E staining of the tumors was also performed (Fig. S2). In addition, DU145-OCT4 cells were significantly more resistant to docetaxel (Fig. 2f). Taken together, these results suggest that the malignant phenotype observed in EOS-selected cells is due to high levels of OCT4 expression.

Identification of ribavirin as a novel drug for treating malignant PCA. The above-mentioned results indicate that the EOS selection system could be used for novel medical screening. Therefore, we tried to identify the candidate compounds that could be used to treat CRPC. We compared the gene expression arrays for PGK- and EOS-selected cells to characterize their molecular signatures and then used *in silico* screening to identify a chemical agent that could reprogram the gene expression signatures of these cells (Fig. 3a). To detect changes in gene expression and to identify EOS signatures, the genes that showed at least a twofold difference in expression levels between the PGK and EOS arrays were used to generate a list of genes with significantly different expression levels (Fig. 3b). The EOS signature was entered into the Connectivity Map, which is a database containing the gene expression profiles of different cells treated with various drugs. We then identified the candidate compounds ($P < 0.05$) that had the potential to reprogram the EOS gene expression signature.[32,33]

Next we examined whether the candidate compounds affected the docetaxel resistance exhibited by DU145-EOS cells (Figs 4a,S3). Acebutolol and Fursultiamine had no effect on DU145-EOS cells (Fig. S3); however, ribavirin-treated DU145-EOS cells were significantly less resistant to docetaxel than non-treated DU145-EOS (Fig. 4a). Next, DU145-EOS tumors (approximately 200 mm^3 in volume) were established in nude mice. The tumor-bearing mice were assigned to five groups: non-treated; docetaxel alone; ribavirin alone; docetaxel plus ribavirin; or docetaxel plus ribavirin (Fig. 4b–e). Docetaxel was injected i.p. on day 1. Ribavirin was given orally on day 1 and then daily thereafter to day 15. The mice treated with both ribavirin and docetaxel showed marked tumor regression, as compared with the mice treated with docetaxel alone (Fig. 4b,c). The tumors excised from the mice treated with ribavirin plus docetaxel showed significantly more tumor cell loss than the tumors treated with docetaxel alone (Fig. 4d,e). Overall, these results indicate that ribavirin reprograms the malignant phenotype of EOS-selected cells through the enhancement of docetaxel efficacy.

Ribavirin reprograms the gene expression signature of DU145-EOS cells. It is important to examine the mechanism underlying the effects of ribavirin on the growth of DU145-EOS tumors. The Connectivity Map identified ribavirin as a compound that could potentially reprogram the EOS gene

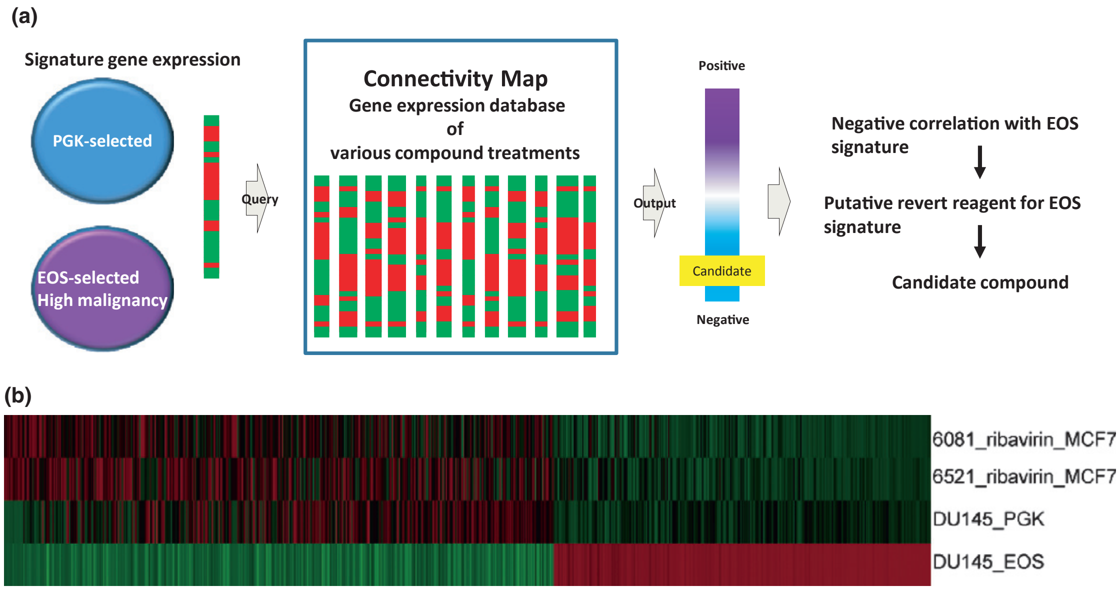

Connectivity Map and cell line	Mean	Enrichment	*P*	Specificity
Acebutolol - MCF7	–0.483	–0.963	0.00304	0
PF-00539758-00 - PC3	–0.352	–0.958	0.00378	0.0083
Fursultiamine - MCF7	–0.391	–0.928	0.01076	0.0126
15(S)-15-methylprostaglandin E2 - PC3	–0.428	–0.924	0.01183	0.0574
Ribavirin - MCF7	–0.402	–0.91	0.01604	0.0135
Oxamniquine - MCF7	–0.375	–0.906	0.01781	0.0123
Meglumine - MCF7	–0.375	–0.889	0.02439	0.0265
Vincamine - PC3	–0.369	–0.854	0.04237	0.0482
Chlorhexidine - PC3	–0.4	–0.845	0.04841	0.0461

Fig. 3. Signature-based screening of candidate chemicals using the Connectivity Map. (a) Simplified scheme showing the strategy used to identify potential chemicals to treat malignant prostate cancer tumors. We evaluated the gene expression signatures of early transposon Oct4 and Sox2 enhancer (EOS)-selected cancer cells and compared them using the Connectivity Map. Drugs showing an inverse gene signature could be used to reprogram EOS-selected cells. (b) Heat map depicting the microarray data derived from DU145-PGK, DU145-EOS and ribavirin-treated MCF7 cells. The data of MCF7 ribavirin were selected through the Connectivity Map as the inverse correlation pattern of the difference between DU145-PGK and DU145-EOS cells (upper). The list of candidate revert compounds (lower).

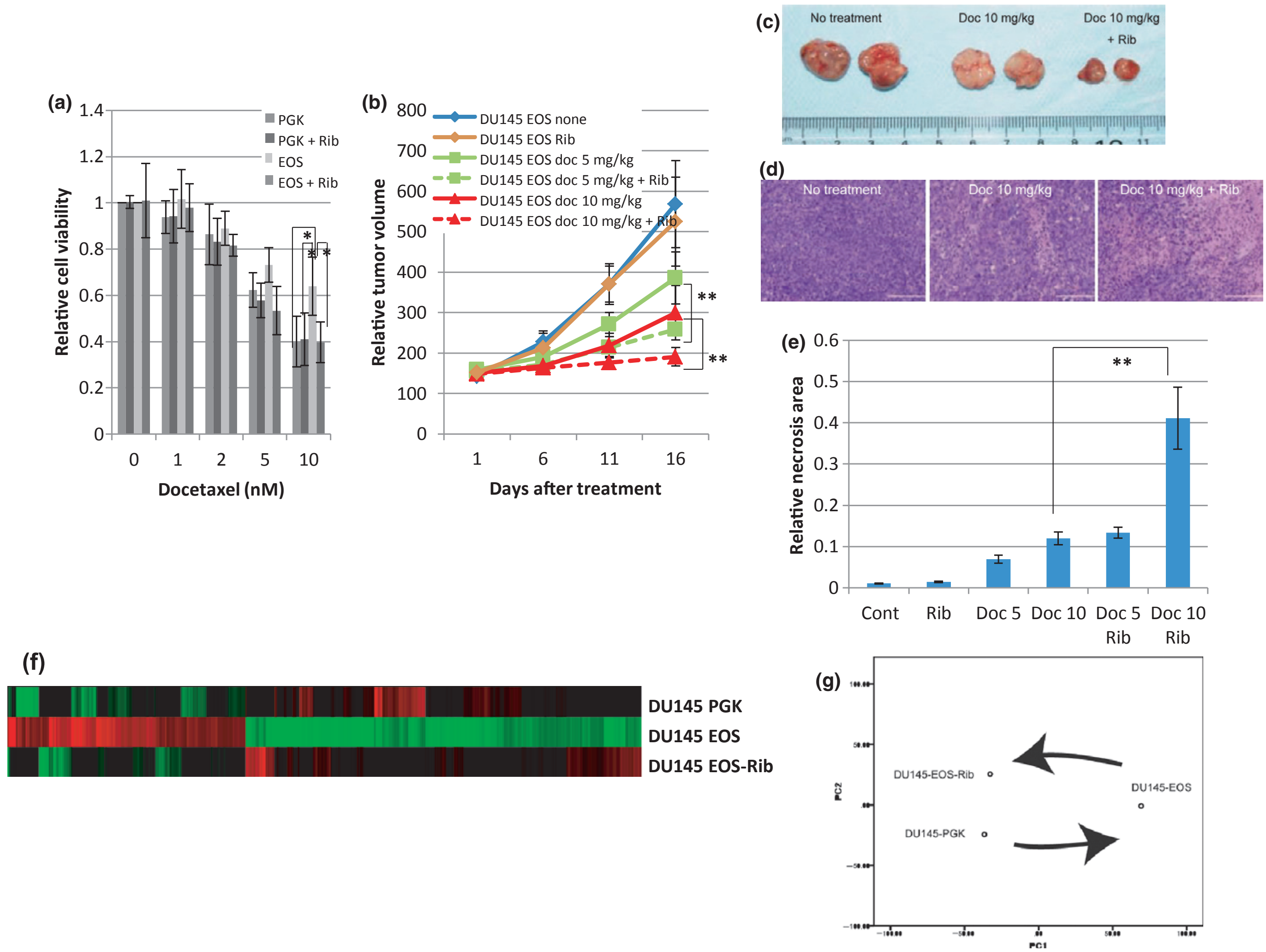

Fig. 4. Ribavirin reprograms malignant DU145-EOS cells. (a) Ribavirin treatment reduced the docetaxel resistance of EOS-selected cells. A water-soluble tetrazolium assay was performed and the viability of EOS-selected cells is shown at the indicated concentrations of docetaxel +/− ribavirin (mean ± SD; $*P < 0.05$). (b) *In vivo* effect of docetaxel +/− ribavirin on DU145-EOS tumors. DU145-EOS cells were injected into nude mice and the mice were treated with docetaxel (5 or 10 mg/kg) either with or without a daily dose of oral ribavirin. The mean tumor volumes are shown at the indicated time points ($n = 6$) (mean ± SD; $**P < 0.01$). (c) DU145-EOS tumors on day 16 after treatment with docetaxel and ribavirin. Two typical cases are shown. (d) H&E staining of DU145-EOS tumors excised on day 16 after drug treatment. Bar, 200 μm. (e) The areas of necrosis were estimated semi-quantitatively (mean ± SD; $**P < 0.01$). (f,g) Microarray analysis of ribavirin-treated EOS cells. Heat map (f) depicting the microarray data and (g) principal component analysis of DU145-PGK, DU145-EOS and DU145-EOS cells treated with ribavirin. EOS, early transposon Oct4 and Sox2 enhancer.

expression signature. To examine whether this was the case, we analyzed the gene expression profile of DU145-EOS cells after ribavirin treatment. A heat map representation of the microarray data and the principal component analysis of DU145-PGK, DU145-EOS and DU145-EOS cells after treatment with ribavirin revealed that ribavirin converted the DU145-EOS gene expression signature into a DU145-PGK gene expression signature (Fig. 4f,g). A quantitative RT-PCR analysis confirmed the downregulation of *OCT4* by ribavirin treatment (Fig. S4). In addition to the qPCR analysis, immunocytochemistry analyses of OCT4 before and after ribavirin treatment showed reduced OCT4 production (Fig. S4). These results indicate that ribavirin was able to reprogram the EOS cells so that they expressed a gene signature similar to that of PGK cells.

Finally, to determine the generality of our findings, we used the EOS system to identify and enrich other PCA cell lines, PC3 and LNCaP cells. LNCaP cells, but not PC3 cells, were enriched with high OCT4 expression by the EOS system (Figs S2,S5,S6,S7). The enriched LNCaP-EOS cells also showed an aggressive phenotype (Figs S2,S5). Ribavirin treatment reduced the tumorigenicity of the LNCaP-EOS cells (Figs S8,S9). These results confirmed that ribavirin is a promising candidate drug for the treatment of docetaxel-resistant PCA.

To understand the effects of ribavirin treatment, we analyzed the microarray data in more detail. First, we focused on the cell cycle genes. Since many antitumor drugs target cell replication, slowly growing cells are potentially drug resistant.[34,35] The EOS gene signature revealed that the cell cycle pathways controlling cell proliferation were repressed (Fig. 5a). Interestingly, ribavirin antagonized the gene expression profiles that mediated slow progression through the cell cycle (Fig. 5b). The fold changes in the expression of each gene are summarized in Table S1. These results indicate that ribavirin can revert the rate of cell cycle progression in EOS cells and reprogram them to be more susceptible to toxic drugs.

doi: 10.1111/cas.12183

Furthermore, from the signature genes (Figs 4f,S8f), we compiled gene lists and performed a pathway analysis (Tables 1, S2, S3). The results indicate that the term cytokine/cytokine receptor interaction was listed in both the upregulated and downregulated conditions by the EOS selection and ribavirin treatment (Table 1). Interestingly, in the list of EOS upregulated but ribavirin downregulated genes, inflammatory cytokines such as IFNγ and IL1α were found (Table S4). Humoral factors reportedly enhance PCA malignancy.[36] In addition, neuroactive ligand/receptor interaction was listed as upregulated by EOS selection and as upregulated and downregulated by ribavirin treatment (Table 1). In the neuroactive ligand receptor interaction, the EOS upregulated but ribavirin downregulated gene was leptin (Table S4). Among neuroactive ligand/receptor interactions, leptin is a key molecule for cell metabolism.[37] Leptin reportedly links tumor-initiating cells through pluripotency-associated transcription factors, including OCT4.[38]

Discussion

Cell fate can be manipulated by the induction of transcription factors. In particular, iPS cell technology allows terminally differentiated somatic cells to be reprogrammed into pluripotent cells.[6,7,39] In addition to iPS cells, neural cells, cardiomyocytes and hepatocytes can be derived from mouse embryonic fibroblasts.[40–42] These dedifferentiation processes are referred to as somatic cell reprogramming and direct reprogramming, respectively. As a result of reprogramming, cells show altered global gene expression patterns, phenotypes and functions. Therefore, we speculated that identifying the global gene expression pattern of a cell would enable its phenotype /function to be reprogrammed. We used this concept to screen a database containing the gene expression patterns of cells treated with different chemical compounds (the Connectivity Map) and identified ribavirin as a candidate drug that could reprogram the malignant phenotype exhibited by PCA tumors.

To obtain malignant PCA tumors, we focused on cells showing high OCT4 expression. *OCT4* encodes a transcription factor that functions in numerous cellular processes, including maintaining embryonic stem cell pluripotency and directing differentiation to particular cell lineages by balancing proliferation and differentiation.[43,44] Thus, deregulated OCT4 expression in PCA cells is likely to perturb normal cellular signaling and favor a transformed phenotype. Intriguingly, consistent

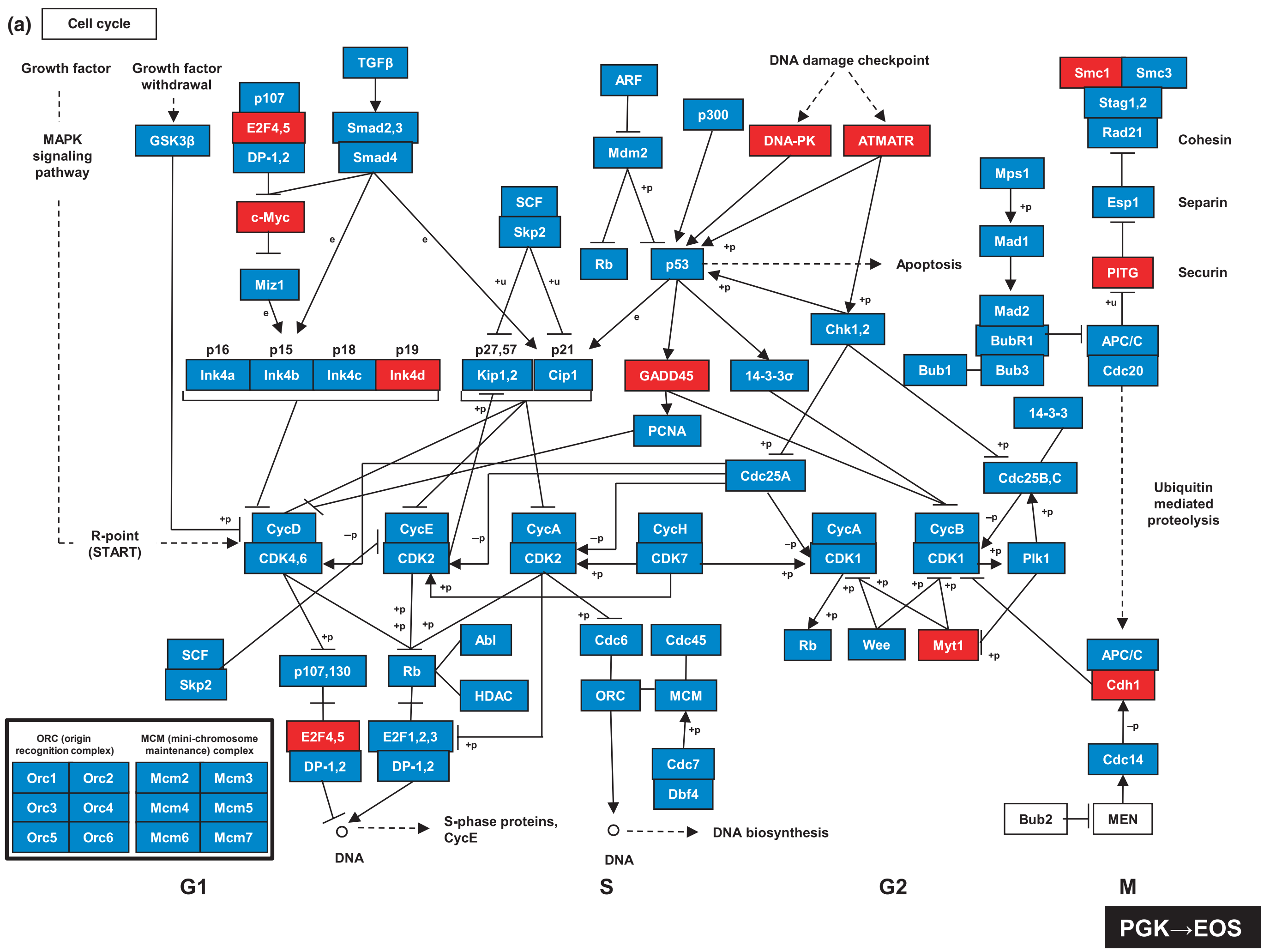

Fig. 5. Ribavirin slows the rate of cell cycle progression in early transposon Oct4 and Sox2 enhancer (EOS) cells and reprograms them to be more susceptible to toxic drugs. (a,b) Gene expression changes in the cell cycle pathways induced by EOS or ribavirin. The diagrams denote the canonical cell cycle pathways derived from the Kyoto Encyclopedia of Genes and Genomes (KEGG) database (http://www.genome.jp/kegg/). Red nodes indicate upregulated genes and blue nodes indicate downregulated genes. (a) Changes in gene expression as cells revert from EOS to PGK. (b) Gene expression changes in EOS cells induced by ribavirin treatment. (c) Simplified schematic showing the strategy used to identify candidate drugs and the concept of drug efficacy reprogramming of cancer cells.

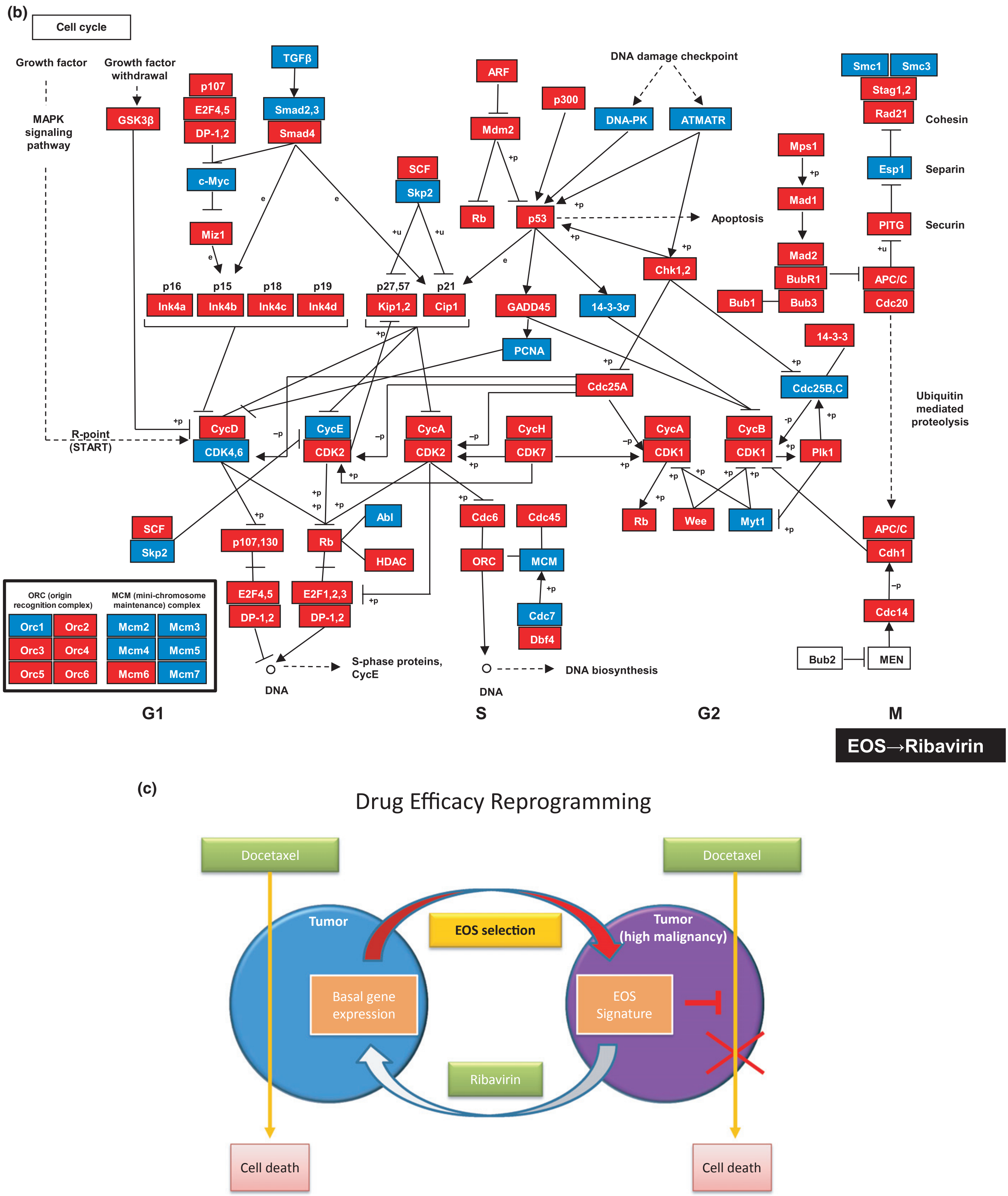

Fig. 5. (Continued)

OCT4 upregulation in human PCA was observed by the expression analysis of the iPS cell inducible 4TF from reported microarray data, including normal prostate, PCA and metastatic prostate cancer (MET) (Fig. S10).[36] These results suggest that among the 4TF OCT4 plays a unique role in PCA development and progression.

The development of chemical genetic screening approaches has enabled the identification of potential small molecule

doi: 10.1111/cas.12183

Table 1. Pathways involved in the early transposon Oct4 and Sox2 enhancer (EOS) and ribavirin signature

Upregulated pathway from PGK to EOS selection	
	KEGG_NEUROACTIVE_LIGAND_RECEPTOR_INTERACTION
	KEGG_CYTOKINE_CYTOKINE_RECEPTOR_INTERACTION
	KEGG_TASTE_TRANSDUCTION
Downregulated pathway from PGK to EOS selection	
	KEGG_STEROID_HORMONE_BIOSYNTHESIS
	KEGG_CYTOKINE_CYTOKINE_RECEPTOR_INTERACTION
	KEGG_METABOLISM_OF_XENOBIOTICS_BY_CYTOCHROME_P450
Upregulated pathway from EOS to ribavirin treatment	
	KEGG_NEUROACTIVE_LIGAND_RECEPTOR_INTERACTION
	KEGG_PRIMARY_BILE_ACID_BIOSYNTHESIS
	KEGG_CYTOKINE_CYTOKINE_RECEPTOR_INTERACTION
Downregulated pathway from EOS to ribavirin treatment	
	KEGG_CYTOKINE_CYTOKINE_RECEPTOR_INTERACTION
	KEGG_NEUROACTIVE_LIGAND_RECEPTOR_INTERACTION
	KEGG_CHEMOKINE_SIGNALING_PATHWAY

drugs; however, high-throughput screens focus on the expression of specific genes rather than on global gene expression patterns.[45] Our findings indicate that drugs that promote the inverse expression of signature genes can be identified from the Connectivity Map and that these drugs might have therapeutic potential. We observed that ribavirin reprogrammed the gene signature of EOS-selected PCA cells, which showed an aggressive malignant phenotype, into a signature resembling that of cells with a much less aggressive phenotype. The concept underlying this strategy, that is, to alter a cell's phenotype by changing its genetic signature, is based on cell reprogramming technology. We propose that this approach, which we named DER (Fig. 5c), can be applied to other types of cancer cells.

Ribavirin shows antiviral activity against several RNA viruses and is used clinically, in combination with interferon-α, to treat hepatitis C infection and as a monotherapy to treat Lassa fever.[46–50] Ribavirin is thought to act by inhibiting 5′ mRNA capping by competing with guanosine for guanyl transferase.[48,51] Recently, it was reported that ribavirin inhibits the growth of human cancer cells.[52–55] Significantly, micromolar plasma concentrations of ribavirin are achievable in humans with minimal toxicity.[55] Our microarray studies revealed the induction of interesting genes, such as *IFN*γ, *IL1*α and *leptin*, which might be involved in tumor suppression through cell signaling and metabolic changes. Therefore, combination therapy with docetaxel and ribavirin is immediately applicable for the treatment of PCA, particularly docetaxel-resistant MET.

Acknowledgments

We thank Drs J. Ellis (University of Toronto) and A. Hotta (Kyoto University) for providing the EOS selection system. We also thank Mr T. Kinoshita (Keio University) for lentivirus production and Dr H. Saya (Keio University) for helpful suggestions and discussions. The present study was supported by PRESTO, of the Japan Science and Technology Agency and Scientific Research (C), and a grant from the Project for Realization of Regenerative Medicine. Support for the core institutes for iPS cell research was provided by MEXT, a Grant-in-Aid for the Global century COE program from MEXT to Keio University and the Keio University Medical Science Fund.

Disclosure Statement

The authors declare no competing financial interests, except for S.S., who is an employee of INFOCOM Corporation.

References

1 Clevers H. The cancer stem cell: premises, promises and challenges. *Nat Med* 2011; **17**: 313–9.
2 Reya T, Morrison SJ, Clarke MF, Weissman IL. Stem cells, cancer, and cancer stem cells. *Nature* 2001; **414**: 105–11.
3 Visvader JE, Lindeman GJ. Cancer stem cells in solid tumours: accumulating evidence and unresolved questions. *Nat Rev Cancer* 2008; **8**: 755–68.
4 Gupta PB, Chaffer CL, Weinberg RA. Cancer stem cells: mirage or reality? *Nat Med* 2009; **15**: 1010–2.
5 Scheel C, Weinberg RA. Phenotypic plasticity and epithelial-mesenchymal transitions in cancer and normal stem cells? *Int J Cancer* 2011; **129**: 2310–4.
6 Takahashi K, Tanabe K, Ohnuki M *et al.* Induction of pluripotent stem cells from adult human fibroblasts by defined factors. *Cell* 2007; **131**: 861–72.
7 Takahashi K, Yamanaka S. Induction of pluripotent stem cells from mouse embryonic and adult fibroblast cultures by defined factors. *Cell* 2006; **126**: 663–76.
8 Miura K, Okada Y, Aoi T *et al.* Variation in the safety of induced pluripotent stem cell lines. *Nat Biotechnol* 2009; **27**: 743–5.
9 Murry CE, Keller G. Differentiation of embryonic stem cells to clinically relevant populations: lessons from embryonic development. *Cell* 2008; **132**: 661–80.
10 Hotta A, Cheung AY, Farra N *et al.* EOS lentiviral vector selection system for human induced pluripotent stem cells. *Nat Protoc* 2009; **4**: 1828–44.
11 Hotta A, Cheung AY, Farra N *et al.* Isolation of human iPS cells using EOS lentiviral vectors to select for pluripotency. *Nat Methods* 2009; **6**: 370–6.
12 Kim JB, Greber B, Arauzo-Bravo MJ *et al.* Direct reprogramming of human neural stem cells by OCT4. *Nature* 2009; **461**: 649–3.
13 Zhu S, Li W, Zhou H *et al.* Reprogramming of human primary somatic cells by OCT4 and chemical compounds. *Cell Stem Cell* 2010; **7**: 651–5.
14 Gidekel S, Pizov G, Bergman Y, Pikarsky E. Oct-3/4 is a dose-dependent oncogenic fate determinant. *Cancer Cell* 2003; **4**: 361–70.
15 Hochedlinger K, Yamada Y, Beard C, Jaenisch R. Ectopic expression of Oct-4 blocks progenitor-cell differentiation and causes dysplasia in epithelial tissues. *Cell* 2005; **121**: 465–77.
16 Tai MH, Chang CC, Kiupel M, Webster JD, Olson LK, Trosko JE. Oct4 expression in adult human stem cells: evidence in support of the stem cell theory of carcinogenesis. *Carcinogenesis* 2005; **26**: 495–502.
17 Gu G, Yuan J, Wills M, Kasper S. Prostate cancer cells with stem cell characteristics reconstitute the original human tumor *in vivo*. *Cancer Res* 2007; **67**: 4807–15.
18 Linn DE, Yang X, Sun F *et al.* A Role for OCT4 in tumor initiation of drug-resistant prostate cancer cells. *Genes Cancer* 2010; **1**: 908–16.
19 Chiou SH, Yu CC, Huang CY *et al.* Positive correlations of Oct-4 and Nanog in oral cancer stem-like cells and high-grade oral squamous cell carcinoma. *Clin Cancer Res* 2008; **14**: 4085–95.
20 Levings PP, McGarry SV, Currie TP *et al.* Expression of an exogenous human Oct-4 promoter identifies tumor-initiating cells in osteosarcoma. *Cancer Res* 2009; **69**: 5648–55.
21 Schoenhals M, Kassambara A, De Vos J, Hose D, Moreaux J, Klein B. Embryonic stem cell markers expression in cancers. *Biochem Biophys Res Commun* 2009; **383**: 157–62.
22 Wolf AM, Wender RC, Etzioni RB, *et al.* American Cancer Society guideline for the early detection of prostate cancer: update 2010. *CA Cancer J Clin* 2010; **60**: 70–98.
23 Freedland SJ. Screening, risk assessment, and the approach to therapy in patients with prostate cancer. *Cancer* 2011; **117**: 1123–35.
24 Berthold DR, Pond GR, Soban F, De Wit R, Eisenberger M, Tannock IF. Docetaxel plus prednisone or mitoxantrone plus prednisone for advanced prostate cancer: updated survival in the TAX 327 study. *J Clin Oncol* 2008; **26**: 242–5.
25 Tannock IF, De Wit R, Berry WR *et al.* Docetaxel plus prednisone or mitoxantrone plus prednisone for advanced prostate cancer. *N Engl J Med* 2004; **351**: 1502–12.
26 Petrylak DP, Tangen CM, Hussain MH *et al.* Docetaxel and estramustine compared with mitoxantrone and prednisone for advanced refractory prostate cancer. *N Engl J Med* 2004; **351**: 1513–20.

27 Ginsberg M, James D, Ding BS *et al.* Efficient direct reprogramming of mature amniotic cells into endothelial cells by ETS factors and TGFbeta suppression. *Cell* 2012; **151**: 559–75.
28 Buganim Y, Itskovich E, Hu YC *et al.* Direct reprogramming of fibroblasts into embryonic Sertoli-like cells by defined factors. *Cell Stem Cell* 2012; **11**: 373–86.
29 Kinoshita T, Nagamatsu G, Kosaka T *et al.* Ataxia-telangiectasia mutated (ATM) deficiency decreases reprogramming efficiency and leads to genomic instability in iPS cells. *Biochem Biophys Res Commun* 2011; **407**: 321–6.
30 Kentsis A, Topisirovic I, Culjkovic B, Shao L, Borden KL. Ribavirin suppresses eIF4E-mediated oncogenic transformation by physical mimicry of the 7-methyl guanosine mRNA cap. *Proc Natl Acad Sci USA* 2004; **101**: 18105–10.
31 Zafarana G, Avery SR, Avery K, Moore HD, Andrews PW. Specific knockdown of OCT4 in human embryonic stem cells by inducible short hairpin RNA interference. *Stem Cells* 2009; **27**: 776–82.
32 Lamb J. The Connectivity Map: a new tool for biomedical research. *Nat Rev Cancer* 2007; **7**: 54–60.
33 Lamb J, Crawford ED, Peck D *et al.* The Connectivity Map: using gene-expression signatures to connect small molecules, genes, and disease. *Science* 2006; **313**: 1929–35.
34 Shah MA, Schwartz GK. Cell cycle-mediated drug resistance: an emerging concept in cancer therapy. *Clin Cancer Res* 2001; **7**: 2168–81.
35 Moncharmont C, Levy A, Gilormini M *et al.* Targeting a cornerstone of radiation resistance: cancer stem cell. *Cancer Lett* 2012; **322**: 139–47.
36 Mimeault M, Batra SK. Development of animal models underlining mechanistic connections between prostate inflammation and cancer. *World J Clin Oncol* 2013; **4**: 4–13.
37 Konner AC, Bruning JC. Selective insulin and leptin resistance in metabolic disorders. *Cell Metab* 2012; **16**: 144–52.
38 Feldman DE, Chen C, Punj V, Tsukamoto H, Machida K. Pluripotency factor-mediated expression of the leptin receptor (OB-R) links obesity to oncogenesis through tumor-initiating stem cells. *Proc Natl Acad Sci USA* 2012; **109**: 829–34.
39 Hanna J, Markoulaki S, Schorderet P *et al.* Direct reprogramming of terminally differentiated mature B lymphocytes to pluripotency. *Cell* 2008; **133**: 250–64.
40 Caiazzo M, Dell'Anno MT, Dvoretskova E *et al.* Direct generation of functional dopaminergic neurons from mouse and human fibroblasts. *Nature* 2011; **476**: 224–7.
41 Ieda M, Fu JD, Delgado-Olguin P *et al.* Direct reprogramming of fibroblasts into functional cardiomyocytes by defined factors. *Cell* 2010; **142**: 375–86.
42 Sekiya S, Suzuki A. Direct conversion of mouse fibroblasts to hepatocyte-like cells by defined factors. *Nature* 2011; **475**: 390–3.
43 Nichols J, Zevnik B, Anastassiadis K *et al.* Formation of pluripotent stem cells in the mammalian embryo depends on the POU transcription factor Oct4. *Cell* 1998; **95**: 379–91.
44 Niwa H, Miyazaki J, Smith AG. Quantitative expression of Oct-3/4 defines differentiation, dedifferentiation or self-renewal of ES cells. *Nat Genet* 2000; **24**: 372–6.
45 Ainsworth C. Networking for new drugs. *Nat Med* 2011; **17**: 1166–8.
46 Davis GL, Esteban-Mur R, Rustgi V *et al.* Interferon alfa-2b alone or in combination with ribavirin for the treatment of relapse of chronic hepatitis C. International Hepatitis Interventional Therapy Group. *N Engl J Med* 1998; **339**: 1493–9.
47 Mangia A, Santoro R, Minerva N *et al.* Peginterferon alfa-2b and ribavirin for 12 vs. 24 weeks in HCV genotype 2 or 3. *N Engl J Med* 2005; **352**: 2609–17.
48 Maag D, Castro C, Hong Z, Cameron CE. Hepatitis C virus RNA-dependent RNA polymerase (NS5B) as a mediator of the antiviral activity of ribavirin. *J Biol Chem* 2001; **276**: 46094–8.
49 McCormick JB, King IJ, Webb PA *et al.* Lassa fever. Effective therapy with ribavirin. *N Engl J Med* 1986; **314**: 20–6.
50 Crotty S, Maag D, Arnold JJ *et al.* The broad-spectrum antiviral ribonucleoside ribavirin is an RNA virus mutagen. *Nat Med* 2000; **6**: 1375–9.
51 Graci JD, Cameron CE. Mechanisms of action of ribavirin against distinct viruses. *Rev Med Virol* 2006; **16**: 37–48.
52 Floryk D, Tollaksen SL, Giometti CS, Huberman E. Differentiation of human prostate cancer PC-3 cells induced by inhibitors of inosine 5′-monophosphate dehydrogenase. *Cancer Res* 2004; **64**: 9049–56.
53 Pettersson F, Yau C, Dobocan MC *et al.* Ribavirin treatment effects on breast cancers overexpressing eIF4E, a biomarker with prognostic specificity for luminal B-type breast cancer. *Clin Cancer Res* 2011; **17**: 2874–84.
54 Kraljacic BC, Arguello M, Amri A, Cormack G, Borden K. Inhibition of eIF4E with ribavirin cooperates with common chemotherapies in primary acute myeloid leukemia specimens. *Leukemia* 2011; **25**: 1197–200.
55 Assouline S, Culjkovic B, Cocolakis E *et al.* Molecular targeting of the oncogene eIF4E in acute myeloid leukemia (AML): a proof-of-principle clinical trial with ribavirin. *Blood* 2009; **114**: 257–60.

Supporting Information

Additional Supporting Information may be found in the online version of this article:

Fig. S1. Immunocytochemistry of OCT4-expressing DU145 cells before and after selection.

Fig. S2. H&E staining of various specimens.

Fig. S3. Acebutolol and fursultiamine have no effect on DU145-EOS cells.

Fig. S4. OCT4 expression in DU145-EOS cells with or without ribavirin treatment.

Fig. S5. Increased expression of OCT4 and enhanced tumorigenicity in EOS-selected LNCaP cells.

Fig. S6. Immunocytochemistry of OCT4-expressing LNCaP cells before and after selection.

Fig. S7. High OCT4 expression increases the malignancy of LNCap cells.

Fig. S8. Ribavirin reprograms the signature gene expression of malignant LNCaP-EOS cells.

Fig. S9. OCT4 expression in LNCaP-EOS cells with or without ribavirin treatment.

Fig. S10. Progression-related analysis of 4TF mRNA expression in human PCA according to reported microarray data.

Table S1. Fold change in the expression of each gene in Figure 5a,b.

Table S2. Factors involved in the EOS signature.

Table S3. Factors involved in the ribavirin signature.

Table S4. Factors involved in the pathway of the EOS and ribavirin signature.

doi: 10.1111/cas.12183